Digital Object Identifier (DOI): 10.1109/INDIN.2015.7281969

2015 IEEE 13th International Conference on Industrial Informatics (INDIN), Cambridge, 2015, pp. 1576-1582.

Control strategies for multi-frequency power transfer in a smart-transformer-fed low-voltage grid

Sebastian Brüske
Giampaolo Buticchi
Marco Liserre

Control Strategies for Multi-Frequency Power Transfer in a Smart-Transformer-Fed Low-Voltage Grid.

Sebastian Brüske, Giampaolo Buticchi and Marco Liserre
Chair of Power Electronics
Christian-Albrechts-Universität zu Kiel
Kaiserstr. 2, 24143 Kiel
Germany
Email: seb@tf.uni-kiel.de

***Abstract*—Smart grids have attracted the attention of the scientific community for years, since the ability to better manage distributed resources in a dynamic grid scenario is of paramount importance. Among the solutions that have been investigated, there is the smart transformer (ST) distribution concept, where an AC/AC power converter substitutes the traditional distribution transformer while enabling additional services. Considering that the ST can generate arbitrary voltage waveforms, power distribution is not restricted anymore to the fundamental frequency, but additional harmonics can be used. This paper analyzes different control possibilities for multi-frequency converters, comparing the results in terms of dynamic performance, control complexity, and communication requirements.**

***Index Terms*—Distributed generation, microgrids, power conditioning, power transmission, power transfer, smart transformer, solid state transformer.**

I. Introduction

Renewable energy exploitation has proved to be a real possibility to face the increasing energy requirement, while trying to address also the environmental issues that comes from fossil-fuel-based electric energy production. However, the increasing penetration of distributed power generation (DPG) such as photovoltaics [1], [2], wind turbine systems [3] and combined heat and power (CHP) [4] systems has heavily affected the medium voltage (MV) and low voltage (LV) grids, impacting mostly on the grid management. In addition, new loads such as electric vehicle charging stations are introduced into the grid. As a result, voltage constraints [5], [6] and line ampacity violations, in addition to a poor power quality (harmonics, flicker, voltage drops) [7], are increasingly present in the distribution grids.

In this framework, the study of decentralized or semi-decentralized grid has received a lot of attention. In particular, micro-grids were intensively studied, and the most advanced approaches aim at implementing in a lower-scale with intelligent converters the hierarchical control that nowadays normally regulate the central power plants [8]. This solution, however, requires that every grid-connected system equipped with a power converter, as grid interface, participate with an important role to the management of the micro-grid. This approach, based on equal sharing of the responsibilities among the players of the micro-grid, entails severe stability and reliability problems [9]–[11]. An intermediate solution, that could be realized in a shorter time with minor stability and reliability challenges but still preserving the advantages of the micro-grid concept, is to gradually switch to smart transformer (ST) distribution. The smart transformer (ST) solution [12] optimally integrates the DPGs and new loads, offering a good power quality and reliability at the same time. The ST is a solid-state transformer, already adopted in railway, harbor, and data center applications. In addition to implementing the step-down conversion, the ST can offer a series of ancillary services to the grid that are otherwise not possible [13], [14].

Even more services can be offered from the ability of the ST to generate arbitrary voltage waveforms at the low-voltage side of the ST, that basically operates as an independent micro-grid. Multi-frequency power transfer (MF-PT) has been recently applied to power electronics. In [15], [16] it is proposed to use an additional frequency in multilevel modular converters (MMC) to implement nestled secondary power loops in order to balance the voltages across the sub-module capacitors, independently of the main power loop. Another field of application is the inductive power transfer (IPT) by means of multiple frequencies [17], where single-frequency pick-ups can be tuned to different transmission frequencies receiving power simultaneously and independently.

In this work, it is hypothesized that the ST generates a voltage with multiple harmonic components on the LV side, feeding a micro-grid, in which traditional loads, designed to operate with only one frequency, and multi-frequency inverters are present. In this context, the power transfer between a power transmitter (T) and a power receiver (R) with the additional frequency component is addressed, and the control possibilities are investigated. In order to avoid interference with the standard equipment T and R have to be well synchronized, which can be realized with or without communication devices. The problem of synchronization will be addressed for a single-phase system, choosing the third harmonic as the additional frequency component.

The focus of this paper is to evaluate the performance of different synchronization methods in this grid scenario. The synchronization of T and R can be achieved by the use of a communication infrastructure. Considering that there are already many industrial products to support communication in

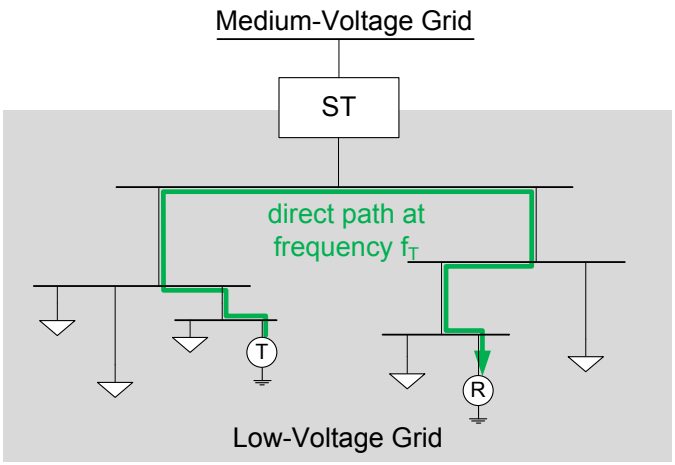

Fig. 1. Multi-frequency operation in a ST based micro-grid where T is the transmitter and R is the receiver

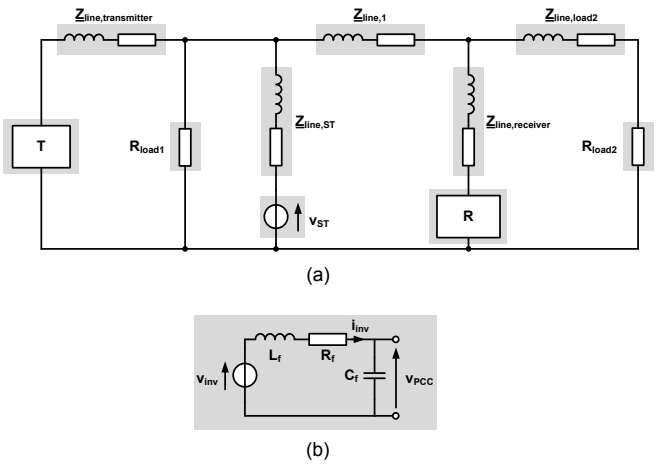

Fig. 2. (a) Circuit of tested LV micro-grid, (b) equivalent circuit of the MF-VSI

smart grids, and considering it is still subject to research [18], it is acceptable to assume that the ST-fed LV grid will feature a communication infrastructure, especially with the multi-frequency inverters. In particular, the availability of power to be transferred with the additional frequency will be signaled to the ST, which will relay this information to the receiver, or vice versa. In this scenario, it will be therefore assumed that the transmitter and the receiver receive synchronized power references, since only a small amount of data needs to be communicated.

A synchronization mechanism between T and the R without a communication infrastructure may be needed if the diffusion of multi-frequency devices happens prior the installation of the communication devices. As a matter of fact, self-synchronizing solutions were presented in literature for single-frequency systems [14], and can be extended to this case. In this way, a method based on droop control between the transmitter and the ST is proposed, meeting the power demand of the receiver.

In Section II, the theory of MF-PT is discussed and two control methods with and without additional communication devices are presented. Based on simulations, a comparison is made in Section III in terms of synchronization effectiveness and control dynamics. Conclusions are finally drawn in Section IV.

II. Control Strategies of Multi-Frequency Inverters

In the following, the theory of MF-PT is briefly explained discussing the idea to apply MF-PT in a LV micro-grid, and a basic control structure for MF-PT is presented. On the basis of this, an extension based on droop-control is proposed in order to achieve synchronization without additional communication devices.

A. Multi-Frequency Power Transfer in LV Micro-Grids

MF-PT is based on the principle of orthogonal power flow, introduced by [15]. The theory states that the different frequency components of non-sinusoidal periodic voltage and current waveforms are orthogonal to each other, leading to the conclusion, that the average power transferred at different frequencies is independent to each other:

$$v(t) = V_0 + \sum_{n=1}^{\infty} \sqrt{2} V_n \cos(n\omega t + \theta_n) \tag{1}$$

$$i(t) = I_0 + \sum_{n=1}^{\infty} \sqrt{2} I_n \cos(n\omega t + \varphi_n)\,. \tag{2}$$

Hence,

$$P = V_0 I_0 + \sum_{n=1}^{\infty} V_n I_n \cos(\theta_n - \varphi_n)\,. \tag{3}$$

In micro-grid operations, this offers the possibility to transfer power point-to-point from a transmitter to a specific receiver by using an additional transmission frequency f_{T}, different from the fundamental frequency [19]. The idea of MF-PT in a ST based micro-grid is shown in Fig.1.

In [19], a current-control (CC) scheme is presented, and the impact of MF-PT on the loads and lines in a distribution network is analyzed, choosing the 3rd harmonic as the additional transmission frequency. As a result, assuming a good synchronization of the transmitter and the receiver, it is possible to stay in compliance with the voltage and current limitations of the grid standards [20], not affecting the local loads but only the lines connecting both the inverters. However, respecting the voltage limitation of a THD of 5% leads to significantly high line currents if a significant amount of power should be transferred. So far, standards for micro-grids, regulating the power quality, have not been determined [21]. This provides the opportunity to think about different harmonic limitations for micro-grids.

The considered single-phase LV micro-grid is shown in Fig.2(a), in which the ST is modeled as a voltage source acting as a slack bus providing voltages at the fundamental and 3rd harmonic frequency. In general, since the ST represents the grid-forming device of the micro-grid, the multi-frequency voltage source inverters (MF-VSI) can be operated as grid-feeding or grid-supporting devices [22]. In this work, the MF-VSIs are operated in grid-feeding mode, wherefore they can be seen as controlled current sources. The inverters are modeled

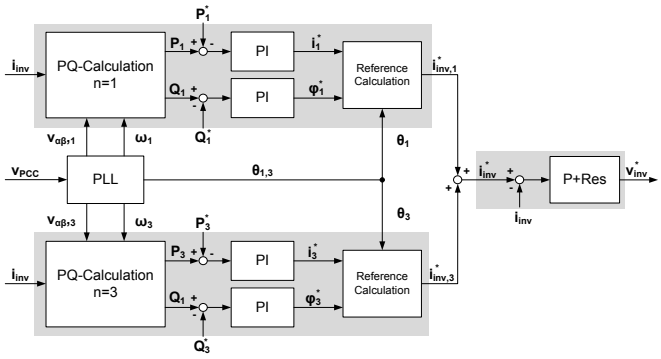

Fig. 3. Current-control strategy of a single-phase MF-VSI

as a voltage source connected through an LC-filter to the point of common coupling (PCC), as depicted in Fig.2(b). In the following, a basic CC scheme is presented, which is suitable for MF-PT in the frame of a communication based (CB) infrastructure for synchronization purposes. This scheme is then extended to the case of a droop based (DB) control, avoiding additional communication devices.

B. Control Strategy in the Frame of a Communication Infrastructure

In general, the control structure of grid-feeding inverters in micro-grids includes an inner current control loop to regulate the injected grid current [22]. The current reference, in turn, is given by an outer power control loop, which is fed by the references of active and reactive power. In the simplest case, a DPG unit is feeding the grid with the maximum available power coming from the generator side, or the power references are set in accordance to the power demand of the grid.

As it is depicted in Fig.3, in case of MF-VSIs, two or more power control loops, one for each transmission frequency, are working in parallel generating the reference of the current at the particular frequency. The power references for the fundamental frequency P_1^* and Q_1^* are determined locally. In contrast, the power references P_3^* and Q_3^* of the 3rd harmonic frequency are set at ST level and transmitted to the MF-VSIs in order to synchronize T and R. The inner control loop is realized by a P+Resonant (PR) controller with harmonic compensator (HC) [23]:

$$G_{\mathrm{PR}}(s) = k_{\mathrm{P}} + k_{\mathrm{I}} \frac{s}{s^2 + \omega_0^2} \tag{4}$$

$$G_{\mathrm{HC}}(s) = \sum_{n=3,5,7,\ldots} k_{\mathrm{I},n} \frac{s}{s^2 + (\omega_0 n)^2}\,. \tag{5}$$

Regularly, the HC is tuned to attenuate the current harmonics of the 3rd, 5th, 7th or higher order harmonics. In case of MF-PT, this ability is used to track the 150 Hz reference instead of compensation purposes.

In order to detect the angles of the grid voltage at 50 Hz and 150 Hz a phase-locked loop (PLL) is needed for each frequency. Additionally, as can be seen from Fig.3, the output of the PLL is used to calculate the current values of the active and reactive power. Since the fundamental and 3rd harmonic frequency are close to each other in the frequency domain, high filtering capabilities are required for the PLL.

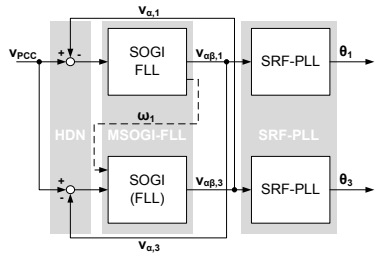

Fig. 4. Block diagram of the MSOGI-FLL PLL with HDN

Therefore, a second order generalized integrator PLL (SOGI-PLL) in synchronous reference frame (SRF) is implemented [24]. The combination of the paralleled SOGI-PLLs and a frequency-locked loop (FLL) results in the frequency adaptive multiple SOGI-FLL (MSOGI-FLL) scheme proposed by [25]. The dynamic behavior of the MSOGI-FLL can be further improved by applying a harmonic decoupling network (HDN) as a cross-feedback to reduce the distortion at the output, which makes the PLL suitable for grid voltages with multiple frequency components. The structure of the PLL is shown in Fig.4. In case of the CB control strategy the ratio between the base frequency and the additional transmission frequency is fixed and ω_1 is used as an input for the SOGI in the branch of the additional frequency. An FLL is not needed to track the frequency ω_3. In case of the DB control strategy the ratio can vary and an FLL has to be implemented in both branches.

In analogy to the filtering of the grid voltage in case of the PLL, the grid current has to be filtered in case of the PQ-calculation. Therefore, a SOGI-based PQ-calculation scheme is implemented [26] in combination with a cross-feedback network:

$$P_n = \frac{1}{2}(v_{\alpha,n} i_{\alpha,n} + v_{\beta,n} i_{\beta,n}) \tag{6}$$

$$Q_n = \frac{1}{2}(v_{\beta,n} i_{\alpha,n} + v_{\alpha,n} i_{\beta,n})\,. \tag{7}$$

C. Control Strategy in the Frame of Droop Control

The presented control scheme can be adapted in order to avoid the use of communication between the ST, T, and R using the well-known droop control concept [27]. By adopting the droop-characteristic of the conventional synchronous generators, power sharing between different DPGs without communication channels can be realized [22]. Since LV grids are mainly resistive, the following droop equations are valid at the fundamental frequency:

$$V - V_0 = -k_{\mathrm{p}}(P - P_0) \tag{8}$$

$$f - f_0 = k_{\mathrm{q}}(Q - Q_0)\,. \tag{9}$$

The R/X-ratio of the grid impedance is decreasing with higher frequencies, resulting in a more and more inductive grid. The network can be mainly inductive at 150 Hz, and therefore the droop characteristics for such grids have to be respected:

$$f_n - f_{0,n} = -k_{\mathrm{p,n}}(P_n - P_{0,n}) \tag{10}$$

$$V_n - V_{0,n} = -k_{\mathrm{q,n}}(Q_n - Q_{0,n})\,. \tag{11}$$

To overcome the uncertainty of the grid behavior a generalized droop-controller can be applied [28], or a virtual impedance

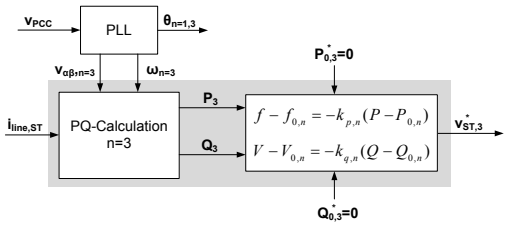

Fig. 5. Droop-control scheme of the ST

scheme can be chosen [29] in order to adapt the control to the grid characteristic.

The idea of the proposed approach is that the voltage of the additional frequency at ST level is regulated by a droop controller. Furthermore, the same droop characteristic is applied to the transmitter for calculating the power reference at this frequency. For the receiver the control structure shown in Fig.3 can be applied. If the receiver sets a power demand at the additional frequency, the ST changes the grid voltage at this frequency following the applied droop characteristic. The transmitter, in turn, reacts on the change of the grid voltage supplying power in order to stabilize the voltage to the reference point. In this way, power sharing between the ST and T is used to synchronize T and R without communication lines.

1) Control of the ST: The ST is modeled as an ideal voltage source with a stiff voltage at the fundamental frequency. The control structure to regulate the voltage at the additional frequency f_{T} is based on (10) and (11) and is shown in Fig.5.

2) Control of the transmitter: For the control of the transmitter the structure of Fig.3 can be used. The only change lies in the calculation of the reference of the active power at the 3rd harmonic frequency P_3^*. The reference is not given directly by the ST, but it is due to the droop-characteristic that is applied to the ST. The control law can be yielded from (10):

$$P_n^* = -\frac{k_n}{k_{\mathrm{p,n}}}(f_n - f_{0,n}) + P_{0,n}\,, \tag{12}$$

where k_n is an additional gain that regulates the ratio of the power sharing between the ST and T. $P_{0,n}$ is set to zero in order to have no power transfer at the additional frequency, if the receiver has no power demand. The reference of reactive power Q_3^* is not used for the droop control and it is set to zero.

III. Simulation Results

In this section, the control strategies described above are applied to the network shown in Fig.1 by simulations. The ST applies voltages at the fundamental and 3rd harmonic frequency to the network ($V_{\mathrm{rms},1} = 230\,V$, $V_{\mathrm{rms},3} = 20\,V$). The loads 1 and 2 are assumed to be constant and purely resistive ($R_{\mathrm{load1}} = 20\,\Omega$, $R_{\mathrm{load2}} = 100\,\Omega$), and the line data are listed in Table I. The two concepts are compared in terms of dynamic performance as well as in terms of synchronization effectiveness. Moreover, the suitability for MF-PT will be discussed. In the first case, both the transmitter (T) and the receiver (R) receive the power references from the ST, whereas in the second case R is setting a power demand and the ST and T share the power due to the gain k_3. The chosen control parameters are listed in Table II.

A. Discussion of the Dynamic Behavior

The two cases with and without communication are shown in Fig.6 and Fig.7, respectively. It can be seen that in both cases T and R have a reference step change to $P^*_{50\mathrm{Hz}} = 1000\,\mathrm{W}$ at $t = 1\,\mathrm{s}$. The references for reactive power are held constant ($Q^*_{50\mathrm{Hz}} = Q^*_{150\mathrm{Hz}} = 0\,\mathrm{VA}$). In the first case, the reference of the active power at 150 Hz of T is changing from zero to $P^*_{150\mathrm{Hz}} = 100\,\mathrm{W}$ at $t = 3\,\mathrm{s}$. The same step with a negative sign is applied to R. This results in three different phases: In the first phase the micro-grid is only fed by the ST, in the second phase neither T nor R provide/drain active power at 150 Hz, and in the third phase T provides and R drains the same amount of active power at 150 Hz. In the second case the simulations result in the same three phases with the difference that only R has a step change of $P^*_{150\mathrm{Hz}}$ at $t = 3\,\mathrm{s}$. The ST and T are following this demand due to their droop characteristic.

Comparing the responses of T to the step changes of $P^*_{150\mathrm{Hz}}$ in Fig.8, it can be seen that the settling time and the overshoot in the first case is lower than the one that results in the second case. Both control strategies offer a satisfying dynamic behavior. Only the response of the ST, shown in Fig.7(c), has an high overshoot of 35%. This and the slower dynamic behavior of T are due to the control principle. At first, only the ST is responding to the power demand of R. Then, T is reacting on the change of the grid voltage, lowering the steady-state power level of the ST. As can be seen in Fig.7(a) and Fig.7(c), the power demand of R is shared between the ST and T resulting in a steady-state error between the power level of T and R. By changing the gain k_3 the power sharing between the ST and T can be varied and thus the steady-state error of the power transmission between T and R can be influenced. In summary, in case of a communication infrastructure, the controller design is a more straightforward approach, caused by the possibility to apply common design rules. In contrast, in case of droop control, it is difficult to find the optimal droop parameters, which lead to a fast yet robust control design. In the DB structure, the ratio between the additional

TABLE I. Line Data

Line	Length (m)	Resistance (mΩ)	Inductance (μH)
Transmitter	200	42.0	50.9
ST	200	42.0	50.9
1	300	63.0	76.4
Receiver	200	42.0	50.9
Load 2	100	21.0	25.5

TABLE II. Control Parameters

Parameter	Communication line based (CB)	Droop control based (DB)
$k_{\mathrm{P,i}}$	13.6	-
$k_{\mathrm{I,i}}$,$k_{\mathrm{I3,i}}$	1000	-
$k_{\mathrm{P,pq}}$	0.0001	0.0001
$k_{\mathrm{I,pq}}$	0.00115	0.00115
k_3	-	1
$k_{\mathrm{p,3}}$	-	0.01
$k_{\mathrm{q,3}}$	-	0.2
k_{SOGI}	0.7	0.7

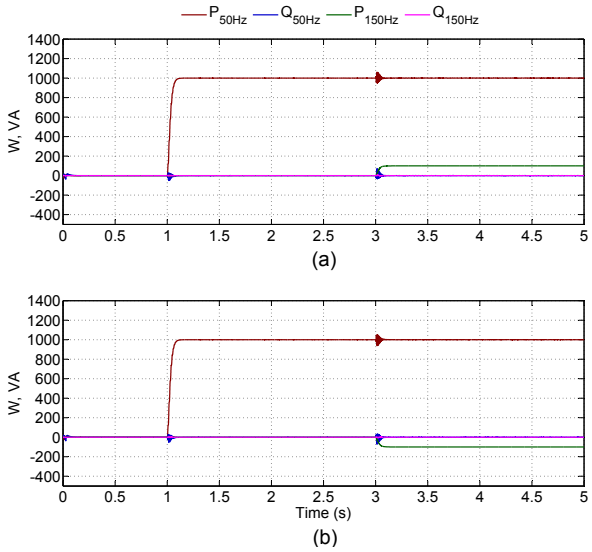

Fig. 6. Active and reactive power in case of CB: (a) transmitter (T), (b) receiver (R).

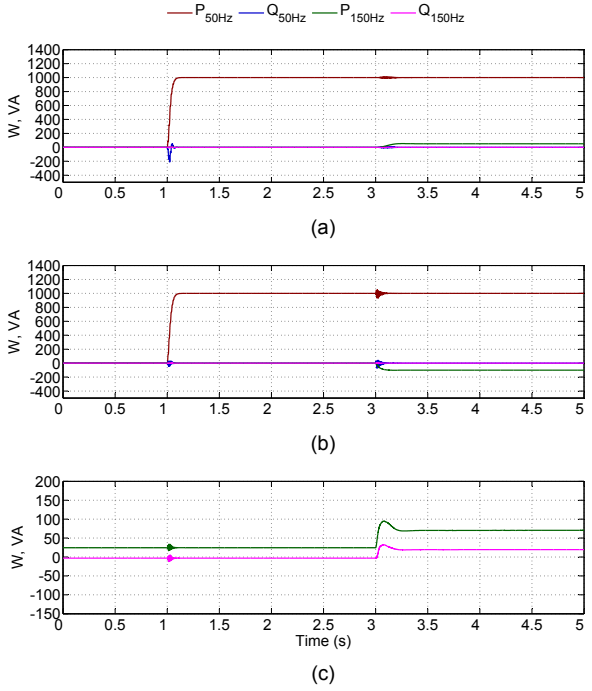

Fig. 7. Active and reactive power in case of DB: (a) transmitter (T), (b) receiver (R), (c) ST.

frequency and the base frequency is not fixed to be a harmonic frequency as it is done in the CB scheme. Because of this, both frequencies have to be tracked by a separate FLL in order to ensure the correct operation of the SOGI blocks inside the PLL and PQ-calculation structures. The FLL gains have to be tuned carefully to guarantee the filtering capabilities of the SOGI and to avoid unwanted oscillations in the power references.

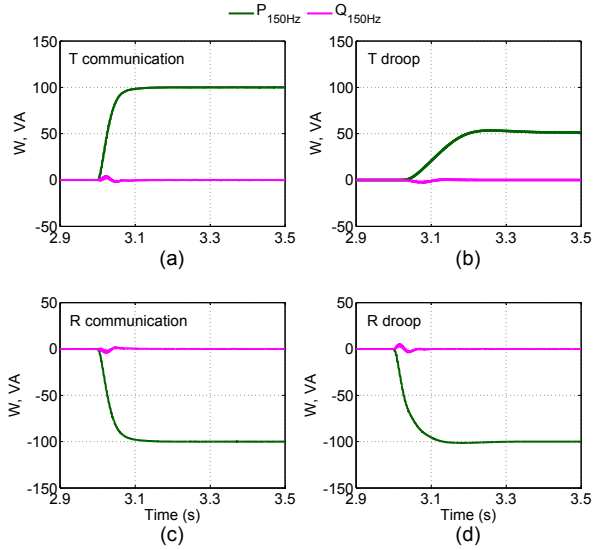

Fig. 8. Comparison of 150 Hz active and reactive power transient: (a) CB: transmitter (T), (b) DB: transmitter (T), (c) CB: receiver (R), (d) DB: receiver (R).

B. Suitability for MF-PT

In order to discuss the suitability for MF-PT the steady-state behavior of the line currents in case of CB and in case of DB for the three phases described above are shown in Fig.9. In the first case it can be seen that, if T and the R have the same power set-point at the 3rd harmonic frequency, the loads and the line at transformer level are not affected by the power transmission. The 150 Hz frequency component of the current at load level is caused by the stiff transformer voltages. The second case shows that power sharing between the ST and T is not affecting the loads, likewise. This leads to the conclusion that both strategies offer the possibility to transmit power point-to-point in the network and are thus suitable for MF-PT.

A fourth phase is shown in Fig.9(e), in which the power set-point of R at 150 Hz is reduced to 75 W. As a consequence, the 150 Hz frequency component of the current at transformer level is almost zero. T becomes the supplier of the current at 150 Hz throughout the grid, whereas ST only provides the voltage of the harmonic frequency. In this way, without knowing all the grid values, the ST can generate a power set-point of the transmitter and the receiver, and ensure a synchronization among them by monitoring the current at transformer level. The same effect can be achieved in the frame of the power sharing method, if the power sharing gain k_3 is varied. This is shown in Fig.9(f) if the gain is set to $k_3 = 4$.

IV. Conclusion

This paper has investigated the possibility to manage power transfer at different frequencies in a smart transformer based distribution grid. The power transfer between a transmitter and a receiver is studied under the hypothesis that a synchronization mechanism between the power reference of the two nodes exists. The other scenario is a synchronization mechanism without a communication infrastructure, for which an approach

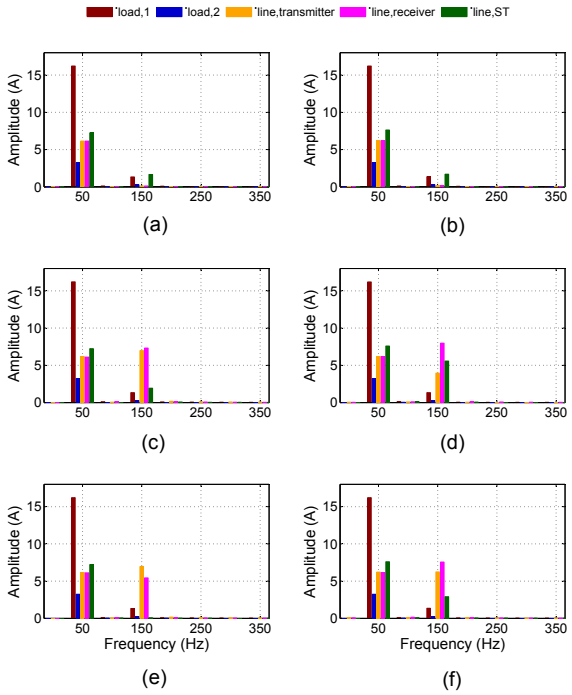

Fig. 9. Spectral analysis of the line currents in cases of CB and DB: (a) only ST feeds the micro-grid (CB), (b) only ST feeds the micro-grid (DB), (c) T transmits and R drains the same amount of power at 150 Hz (CB), (d) R demands power at 150 Hz ST and T share equally (DB), (e) T transmits 100 W and R drains 75 W at 150 Hz (CB), (f) R demands power at 150 Hz ST and T share differently (DB).

based on droop control has been chosen extending it to the multi-frequency case.

The current control, generally adopted for grid-connected inverters, and the droop control method, adopted in decentralized scenarios, are compared with simulations. The result shows that the current controller is a more straight-forward design and results in a faster dynamic response. The droop controller, however, may still retain interest for communication-less smart grid, where a self-synchronization between generation and consumption is important.

ACKNOWLEDGMENT

The research leading to these results has received funding from the Alexander von Humboldt Foundation.

REFERENCES

[1] M. Thomson and D. Infield, "Impact of widespread photovoltaics generation on distribution systems," *IET Renewable Power Generation*, vol. 1, no. 1, pp. 33–40, Mar. 2007.

[2] A. Canova, L. Giaccone, F. Spertino, and M. Tartaglia, "Electrical impact of photovoltaic plant in distributed network," *IEEE Trans. Ind. Appl.*, vol. 45, no. 1, pp. 341–347, Jan. 2009.

[3] P. Eriksen *et al.*, "System operation with high wind penetration," *IEEE Power and Energy Magazine*, vol. 3, no. 6, pp. 65–74, Nov. 2005.

[4] E. Coster *et al.*, "Integration issues of distributed generation in distribution grids," *Proc. IEEE*, vol. 99, no. 1, pp. 28–39, Jan. 2011.

[5] C. Schwaegerl, M. Bollen, K. Karoui, and A. Yagmur, "Voltage control in distribution systems as a limitation of the hosting capacity for distributed energy resources," in *18th Int. Con. and Exhibition Electricity Distribution (CIRED 2005)*, Jun. 2005, pp. 1–5.

[6] E. De Jaeger, A. Du Bois, and B. Martin, "Hosting capacity of lv distribution grids for small distributed generation units, referring to voltage level and unbalance," in *22nd Int. Conf. and Exhibition Electricity Distribution (CIRED 2013),*, Jun. 2013, pp. 1–4.

[7] E. Muljadi and H. McKenna, "Power quality issues in a hybrid power system," *IEEE Trans. Ind. Appl.*, vol. 38, no. 3, pp. 803–809, May 2002.

[8] J. Guerrero, J. Vasquez, J. Matas, L. de Vicua, and M. Castilla, "Hierarchical control of droop-controlled ac and dc microgrids. a general approach toward standardization," *IEEE Trans. Ind. Electron.*, vol. 58, no. 1, pp. 158–172, Jan. 2011.

[9] A. Bhowmik, A. Maitra, S. Halpin, and J. Schatz, "Determination of allowable penetration levels of distributed generation resources based on harmonic limit considerations," *IEEE Trans. Power Del.*, vol. 18, no. 2, pp. 619–624, Apr. 2003.

[10] V. Quezada, J. Abbad, and T. Román, "Assessment of energy distribution losses for increasing penetration of distributed generation," *IEEE Trans. Power Syst.*, vol. 21, no. 2, pp. 533–540, May 2006.

[11] E. Sortomme, S. Venkata, and J. Mitra, "Microgrid protection using communication-assisted digital relays," *IEEE Trans. Power Del.*, vol. 25, no. 4, pp. 2789–2796, Oct. 2010.

[12] R. Pena-Alzola, G. Gohil, L. Mathe, M. Liserre, and F. Blaabjerg, "Review of modular power converters solutions for smart transformer in distribution system," in *IEEE Energy Conversion Congr. and Expo. (ECCE 2013)*, Sept. 2013, pp. 380–387.

[13] G. De Carne, M. Liserre, K. Christakou, and M. Paolone, "Integrated voltage control and line congestion management in active distribution networks by means of smart transformers," in *IEEE 23rd Int. Symp. Industrial Electronics (ISIE 2014)*, Jun. 2014, pp. 2613–2619.

[14] G. Buticchi, M. Liserre, D. Barater, C. Concari, A. Soldati, and G. Franceschini, "Frequency-based control of a micro-grid with multiple renewable energy sources," in *IEEE Energy Conversion Congr. and Expo. (ECCE 2014)*, Sept. 2014, pp. 5273–5280.

[15] J. Ferreira, "The multilevel modular dc converter," *IEEE Trans. Power Electron.*, vol. 28, no. 10, pp. 4460–4465, Oct. 2013.

[16] ——, "Nestled secondary power loop in multilevel modular converters," in *IEEE 15th Workshop Control and Modeling for Power Electronics (COMPEL 2014)*, Jun. 2014, pp. 1–9.

[17] Z. Pantic, K. Lee, and S. Lukic, "Inductive power transfer by means of multiple frequencies in the magnetic link," in *IEEE Energy Conversion Congr. and Expo. (ECCE 2013)*, Sept. 2013, pp. 2912–2919.

[18] S. Galli, A. Scaglione, and Z. Wang, "For the grid and through the grid: The role of power line communications in the smart grid," *Proc. IEEE*, vol. 99, no. 6, pp. 998–1027, Jun. 2011.

[19] S. Brueske, G. de Carne, and M. Liserre, "Multi-frequency power transfer in a smart transformer based distribution grid," in *40th Ann. Conf. IEEE Industrial Electronics Society (IECON 2014)*, 2014.

[20] *IEEE Standard for Interconnecting Distributed Resources with Electric Power Systems*, IEEE Std 1547-2003 Std., July 2003.

[21] *IEEE Guide for Design, Operation, and Integration of Distributed Resource Island Systems with Electric Power Systems*, Std., July 2011.

[22] J. Rocabert, A. Luna, F. Blaabjerg, and P. Rodriguez, "Control of power converters in ac microgrids," *IEEE Trans. Power Electron.*, vol. 27, no. 11, pp. 4734–4749, Nov. 2012.

[23] R. Teodorescu, F. Blaabjerg, M. Liserre, and P. Loh, "Proportional-resonant controllers and filters for grid-connected voltage-source converters," *Proc. Inst. Elect. Eng.–Elect. Power Appl.*, vol. 153, no. 5, pp. 750–762, Sept. 2006.

[24] M. Ciobotaru, R. Teodorescu, and F. Blaabjerg, "A new single-phase pll structure based on second order generalized integrator," in *37th IEEE Power Electronics Specialists Conf. (PESC'06)*, Jun. 2006, pp. 1–6.

[25] P. Rodriguez, A. Luna, I. Candela, R. Mujal, R. Teodorescu, and F. Blaabjerg, "Multiresonant frequency-locked loop for grid synchronization of power converters under distorted grid conditions," *IEEE Trans. Ind. Electron.*, vol. 58, no. 1, pp. 127–138, Jan. 2011.

[26] Y. Yang and F. Blaabjerg, "A new power calculation method for single-phase grid-connected systems," in *IEEE Int.Symp. Industrial Electronics (ISIE)*, May 2013, pp. 1–6.

[27] R. Brandt, "Theoretical approach to speed and tie line control," *Trans.*

American Institute of Electrical Engineers, vol. 66, no. 1, pp. 24–30, Jan. 1947.

[28] Q.-C. Zhong, "Harmonic droop controller to reduce the voltage harmonics of inverters," *IEEE Trans. Ind. Electron.*, vol. 60, no. 3, pp. 936–945, Mar. 2013.

[29] X. Yu, A. Khambadkone, H. Wang, and S. Terence, "Control of parallel-connected power converters for low-voltage microgrid - part 1: A hybrid control architecture," *IEEE Trans. Power Electron.*, vol. 25, no. 12, pp. 2962–2970, Dec. 2010.